

# Lefschetz Thimble Quantum Monte Carlo for Spin Systems

T. C. Mooney,<sup>1,2</sup> Jacob Bringewatt,<sup>3,4</sup> and Lucas T. Brady<sup>2,3,4</sup>

<sup>1</sup>*George Mason University, Fairfax, Virginia 22030, USA*

<sup>2</sup>*National Institute of Standards and Technology, Gaithersburg, Maryland 20899, USA*

<sup>3</sup>*Joint Center for Quantum Information and Computer Science,  
NIST/University of Maryland, College Park, Maryland 20742, USA*

<sup>4</sup>*Joint Quantum Institute, NIST/University of Maryland, College Park, Maryland 20742, USA*

(Dated: October 22, 2021)

Monte Carlo simulations are often useful tools for modeling quantum systems, but in some cases they suffer from a sign problem, which manifests as an oscillating phase attached to the probabilities being sampled. This sign problem generally leads to an exponential slow down in the time taken by a Monte Carlo algorithm to reach any given level of accuracy, and it has been shown that completely solving the sign problem for an arbitrary quantum system is NP-hard. However, a variety of techniques exist for mitigating the sign problem in specific cases; in particular, the technique of deforming the Monte Carlo simulation's plane of integration onto Lefschetz thimbles (that is, complex hypersurfaces of stationary phase) has seen success for many problems of interest in the context of quantum field theories. We extend this methodology to discrete spin systems by utilizing spin coherent state path integrals to re-express the spin system's partition function in terms of continuous variables. This translation to continuous variables introduces additional challenges into the Lefschetz thimble method, which we address. We show that these techniques do indeed work to lessen the sign problem on some simple spin systems.

The sign problem in quantum Monte Carlo (QMC) is a major impediment to efficiently simulating quantum systems classically. While the sign problem is basis dependent, it is NP-hard, in general, to find a basis with no sign problem [1, 2]. Still, there are numerous heuristic strategies for solving the sign problem in specific cases [3, 4], or mitigating it in others, reducing the severity of the exponential slow down without eliminating it [5, 6].

The sign problem arises via the protocol of reweighting, in which one pushes the quantum quasiprobability distribution's phase onto the observable in order to get proper probabilities with which to conduct Monte Carlo simulations. Specifically, for some (complex) quasiprobability distribution  $\rho = pe^{i\theta}$ , we have that the expectation value of an observable  $O$  is given by:

$$\langle O \rangle_\rho = \frac{\langle O e^{i\theta} \rangle_p}{\langle e^{i\theta} \rangle_p}. \quad (1)$$

This reweighting allows non-positive and non-real quasiprobabilities to be sampled from via Monte Carlo methods, but the method falls apart when the phase is highly oscillatory. This is the case because for a Monte Carlo sampling of an  $n$ -particle system repeated  $m$  times, the relative error in the phase can be written as

$$\Delta e^{i\theta} / \langle e^{i\theta} \rangle_p = e^{\mathcal{O}(\beta n)} / \sqrt{m}, \quad (2)$$

where  $\Delta e^{i\theta}$  is the standard deviation of  $e^{i\theta}$  and  $\beta$  is the inverse temperature [1]. Thus, to keep a constant level of relative error in the Monte Carlo simulation,  $m$  must scale exponentially with both particle number and inverse temperature, neither of which is desirable.

The sign problem can be avoided by Hamiltonians that are stoquastic (where all the off-diagonal entries are real

and non-positive) [7] or, more generally, by Hamiltonians that are in Vanishing Geometric Phase form [8, 9]. In a quantum computing context, stoquastic Hamiltonians play into quantum complexity theory [10, 11]. In adiabatic quantum computing specifically, there is a large body of evidence that local sign-problem free Hamiltonians do not possess quantum advantage over classical computing [12, 13] and that quantum advantage with stoquastic Hamiltonians requires contrived non-local systems [14].

Adiabatic quantum computation with general Hamiltonians is known to be universal [15], and therefore, it is expected that the quantum advantage over classical computation arises for Hamiltonians that exhibit a sign problem. Nonetheless, many classical techniques are known to address the sign problem in certain instances, motivating us to consider for which Hamiltonians the sign problem makes classical simulation truly intractable. More broadly, classically simulating arbitrary many-body quantum systems with sign problems is of general interest.

Lefschetz thimble methods, based on Picard-Lefschetz theory [16], are one promising strategy for mitigating the sign problem [17, 18]. These methods are a higher dimensional analogue of the stationary phase method, deforming an integral into complex space so that it sits on a manifold of stationary phase. This mostly eliminates the rapid phase oscillations which lead to the sign problem.

This approach has primarily been developed in the context of quantum field theories, both bosonic [19–24] and fermionic [25–32]. Most such field theoretic problems are immediately amenable to the Lefschetz thimble approach, as the relevant variables are continuous and, thus, easily complexified. The approach has also

been applied to the Hubbard model [33–35], where prior to applying the techniques one must map the discrete partition function to a functional integral over continuous variables via a Hubbard-Stratonovich transformation [36, 37]. Similarly, for spin systems, one must also map the problem to continuous variables. This was recently done by mapping spins onto complex fermions, but this approach was limited to 2-body interactions between spin-1/2 particles [38].

In this Letter, we adapt Lefschetz thimble Monte Carlo methods to generic spin systems by utilizing spin coherent states to map the partition function for a spin system into a continuous variable setting. Using these continuous variable models for spin, we implement a Lefschetz thimble method to mitigate the sign problem in these spin systems. This provides a potential path toward simulating a larger array of quantum systems using classical methods.

*Lefschetz Thimbles.*—Consider an integral of the form

$$\mathcal{Z} = \int_{\mathbb{R}^n} d^n \mathbf{x} e^{-\mathcal{S}(\mathbf{x})}, \quad (3)$$

where, here,  $n$  is the number of degrees of freedom,  $\mathbf{x} \in \mathbb{R}^n$  (boldface denotes a vector) are the state variables, and  $\mathcal{S}$  is the action. For a complex action  $\mathcal{S}$ , this integrand can be highly oscillatory, and, therefore, can suffer from the sign problem when numerically integrated via QMC. The core of the Lefschetz thimble approach to mitigating this sign problem is to promote  $\mathcal{S}(\mathbf{x}) : \mathbb{R}^n \rightarrow \mathbb{C}$ , to a holomorphic function  $\mathcal{S}(\mathbf{z}) : \mathbb{C}^n \rightarrow \mathbb{C}$ , and deform the original integration region, called an *n-cycle*, to a collection of cycles of stationary phase for the action, on which the imaginary part of the action is constant. On such stationary phase cycles, called *Lefschetz thimbles*, there is no sign problem.

To formally define the stationary phase cycles and to systematize deformation into them, we introduce the concept of a *holomorphic flow*. Let  $\tau$  be the flow-time parameter, a non-physical parameterization of our deformation in the complex hyperplane. We write the result of flowing an initial integration point,  $\mathbf{z}_0$ , for flow-time  $\tau$  as  $\varphi(\mathbf{z}_0; \tau) : \mathbb{C}^n \times \mathbb{R} \rightarrow \mathbb{C}^n$ . Letting  $\mathbf{z}(\tau) \equiv \varphi(\mathbf{z}_0; \tau)$ , we define the holomorphic flow via the differential equation

$$\frac{dz_i}{d\tau} = \overline{\frac{\partial \mathcal{S}}{\partial z_i}}, \quad (4)$$

where the bar denotes complex conjugation. There are a few important things to note about Eq. (4). First, the holomorphic flow is such that the real part of the action monotonically increases under the flow, whereas the imaginary part of the action is constant. This can be confirmed by observing that

$$\frac{d\mathcal{S}}{d\tau} = \sum_i \frac{\partial \mathcal{S}}{\partial z_i} \frac{dz_i}{d\tau} = \sum_i \frac{\partial \mathcal{S}}{\partial z_i} \overline{\frac{\partial \mathcal{S}}{\partial z_i}} \geq 0,$$

and that  $d\mathcal{S}/d\tau$  is real. Alternatively one could simply observe that the holomorphic flow is: (a) the gradient flow of  $\text{Re } \mathcal{S}$ , and, therefore, it is the path of steepest ascent for  $\text{Re } \mathcal{S}$ ; and (b) the Hamiltonian flow for a “Hamiltonian” given by  $\text{Im } \mathcal{S}$ , and, consequently,  $\text{Im } \mathcal{S}$  is conserved under the flow. Second, the critical points of the action (i.e., where  $\partial \mathcal{S} / \partial z_i = 0$  for all  $i$ ) are stationary under the flow. Finally, the Jacobian  $J$  corresponding to the change of variables  $\mathbf{z}_0 \rightarrow \varphi(\mathbf{z}_0; \tau)$  satisfies its own flow equation,

$$\frac{dJ}{d\tau} = \overline{HJ}, \quad (5)$$

where  $H = \left[ \frac{\partial^2 \mathcal{S}}{\partial z_i \partial z_j} \right]$  is the Hessian of  $\mathcal{S}$ .

The flow equations allows us to formally define two interrelated stationary phase *n-cycles*: the *Lefschetz thimble*, and the *anti-thimble*. Let  $\{p_\sigma | \sigma \in \Sigma\}$  be the collection of critical points of  $\mathcal{S}$ , with some indexing set  $\Sigma$ . Then, we can define the *Lefschetz thimble attached to  $p_\sigma$* , denoted  $\mathcal{J}_\sigma$ , to be the collection of all points that flow away from  $p_\sigma$  under Eq. (4). Mathematically:

$$\mathcal{J}_\sigma = \{\mathbf{z} | \varphi(\mathbf{z}; -\infty) = p_\sigma\}. \quad (6)$$

Similarly, *anti-thimble attached to  $p_\sigma$* , written  $\mathcal{K}_\sigma$ , is defined as the set of all points that flow to  $p_\sigma$ . That is:

$$\mathcal{K}_\sigma = \{\mathbf{z} | \varphi(\mathbf{z}; \infty) = p_\sigma\}. \quad (7)$$

Notice that  $\mathcal{J}_\sigma$ , in addition to being a stationary phase cycle of  $\mathcal{S}$ , is also the steepest ascent cycle of  $\mathcal{S}$  from  $p_\sigma$ . This means that we know definitively that  $\mathcal{J}_\sigma$  is a convergent integration cycle for  $e^{-\mathcal{S}}$ , as the boundaries of the integral go to zero as quickly as possible. On the other hand,  $\mathcal{K}_\sigma$  is a cycle of steepest descent, and, therefore, divergent.

The anti-thimbles  $\mathcal{K}_\sigma$  serve their purpose, however, by helping to identify the set of thimbles  $\mathcal{J}_\sigma$  that correspond to our initial integration contour  $\mathbb{R}^n$ . In particular, if some modest conditions are met [16, 18], the integral of  $e^{-\mathcal{S}}$  over any convergent integration cycle can be deformed into an integral over a linear combination of  $\mathcal{J}_\sigma$ s. Given our initial integration cycle  $\mathbb{R}^n$  we have that

$$\mathbb{R}^n \simeq \sum_{\sigma'} \langle \mathcal{K}_{\sigma'}, \mathbb{R}^n \rangle \mathcal{J}_{\sigma'} \quad (8)$$

up to equality of integration, where  $\langle A, B \rangle$  is the intersection pairing of *n-cycles*  $A$  and  $B$ , i.e. the number of isolated intersections between  $A$  and  $B$ .

Provided we can appropriately identify (or approximately identify) the correct intersection pairings, Eq. (8) provides us a pathway to ameliorating the sign problem by integrating over the appropriate linear combination of Lefschetz thimbles instead of  $\mathbb{R}^n$ . While a variety of numerical treatments have shown this approach to be

useful in numerous contexts [21, 27–29, 39–42], it is important to emphasize that this change of integration contour does not fully solve the sign problem. One limitation is that, during the deformation process, the phase of the integrand will pick up a contribution from the Jacobian (the so-called residual phase), which may introduce a sign problem of its own [19, 43]. Furthermore, if multiple thimbles contribute to the partition function, a sign problem can still arise due to the presence of relative phases between different thimbles; such relative phases arise because, while  $\text{Im } \mathcal{S}$  is constant on individual thimbles, it is not so between different thimbles [43]. Despite these caveats, in many cases of interest these issues have not been fatal and the Lefschetz thimble approach has seen great success [19–35, 38], motivating its further application to sign problems in spin systems.

*Algorithms*—Now that we have introduced an analytic framework for addressing the sign problem, we consider the use of Lefschetz thimbles in QMC algorithms. A number of such algorithms have been proposed [21, 27–29, 39–42]; here we consider a particular approach called the *generalized thimble method*, first proposed in Ref. [40]. This algorithm is of particular interest since it does not require *a priori* knowledge of the critical points of the action in the complexified space, and, in principle, guarantees sampling over all relevant thimbles.

The key to this algorithm is the observation that

$$\varphi(\mathbb{R}^n; \infty) = \sum_{\sigma'} \langle \mathcal{K}_{\sigma'}, \mathbb{R}^n \rangle \mathcal{J}_{\sigma'}, \quad (9)$$

which can be intuitively understood by noting that the only structures that the flow can “get stuck” on are the thimbles, and all points not flowing to the thimbles will flow out to infinity, where they, too, will eventually arrive at the thimbles. Thus, for some sufficiently large time  $\tau$ , a flow of  $\mathbb{R}^n$  will approach the appropriate ensemble of thimbles, ameliorating the sign problem. With this in mind, we present the full algorithm:

---

**Algorithm 1** Generalized thimble method

---

**Require:**  $N, \tau \geq 0, \mathbf{z} \in \mathbb{R}^n$ .

- 1:  $\mathbf{z}' = \varphi(\mathbf{z}; \tau)$
- 2:  $\mathcal{S}_{\text{eff}} = \mathcal{S}(\mathbf{z}') - \log \det J$
- 3: **for**  $i \in [0, N) \cap \mathbb{Z}$  **do**
- 4:    $\mathbf{z}_{\text{next}} = \mathbf{z} + \delta \mathbf{z}$ ,  $\delta \mathbf{z}$  random, symmetric
- 5:    $\mathbf{z}'_{\text{next}} = \varphi(\mathbf{z}; \tau)$
- 6:    $\mathcal{S}_{\text{eff,next}} = \mathcal{S}(\mathbf{z}'_{\text{next}}) - \log \det J_{\text{next}}$
- 7:   **if**  $\text{UniformRandom}(0, 1) \leq e^{-(\mathcal{S}_{\text{eff,next}} - \mathcal{S}_{\text{eff}})}$  **then**
- 8:      $\mathbf{z} = \mathbf{z}_{\text{next}}$
- 9:      $\mathbf{z}' = \mathbf{z}'_{\text{next}}$
- 10:     $\mathcal{S}_{\text{eff}} = \mathcal{S}_{\text{eff,next}}$
- 11:   **end if**
- 12:   Record  $\mathbf{z}, \mathbf{z}', \mathcal{S}_{\text{eff}}$ .
- 13: **end for**

---

This algorithm is a Metropolis-Hastings algorithm, with samples taken according to the probability distri-

bution  $e^{-\mathcal{S}_{\text{eff}}}$  on the thimbles, taking into account the requisite change of variables. The larger  $\tau$  is the more multipolar the probability landscape will be, and thus the less effective this algorithm will be in arriving at the desired distribution. As such, there emerge conflicting incentives to both minimize and maximize  $\tau$ , which implies there will be an optimal  $\tau$  balancing these desired outcomes.

It should also be noted that calculating  $\det J$  is by far the most computationally expensive aspect of this algorithm. In this work, we take the approach of simply numerically integrating Eq. (5), but more efficient schemes exist in the literature [24, 42, 44].

*Spin Coherent State Path Integrals.*—While Lefschetz thimble Monte Carlo has been shown to be effective in ameliorating the sign problem, it only works with partition functions expressed as integrals, not the sums seen in standard path integral QMC for spin systems. To apply Lefschetz thimble Monte Carlo to spin systems, we need to write the spin partition function as an actual integral. This can be accomplished using a resolution of the identity expressible as an integral. Spin coherent states provide one such resolution. The novel application of Lefschetz thimble Monte Carlo to spin systems in a general way via spin coherent states is the key result of this Letter.

We define a generic spin- $S$  spin coherent state as

$$|\mu\rangle \equiv \frac{1}{(1 + |\mu|^2)^S} \exp\{\mu \hat{S}_-\} |\uparrow\rangle, \quad (10)$$

where  $\hat{S}_- \equiv \hat{S}_x - i\hat{S}_y$  is the lowering operator,  $|\uparrow\rangle$  is the  $+S$  state in the  $z$ -direction, and  $\mu \in \mathbb{C}$ . Let  $\mu = e^{i\varphi} \tan \theta/2$ ; then  $|\mu\rangle$  corresponds to the  $+S$  eigenstate of the spin operator along an axis rotated from  $+z$  by  $\theta$  about the  $y$ -axis and then  $\varphi$  about the  $z$ -axis [45]. Importantly, spin coherent states can resolve the identity as

$$I = \frac{2S+1}{\pi} \int_{\mathbb{R}^2} \frac{d^2\mu}{(1 + |\mu|^2)^2} |\mu\rangle \langle \mu|, \quad (11)$$

where, for brevity, we let  $d^2\mu := d(\text{Re } \mu)d(\text{Im } \mu)$ .

Let  $\mu_j = x_j + iy_j$  at each “imaginary time-slice”  $j \in \{0 \dots T-1\}$  of the usual path integral. Inserting Eq. (11) at each time-slice, we obtain the discrete *spin coherent state path integral* up to  $\mathcal{O}(\beta/T)$

$$\mathcal{Z} = \left( \prod_{j=0}^{T-1} \frac{2S+1}{\pi} \int_{\mathbb{R}^2} \frac{dx_j dy_j}{(1 + x_j^2 + y_j^2)^2} \right) e^{-\mathcal{S}[\{x_j\}, \{y_j\}]} \quad (12)$$

where

$$\begin{aligned} \mathcal{S}[\{x_j\}, \{y_j\}] \equiv & \sum_{j=0}^{T-1} \left( 2iS \frac{((y_{j+1} - y_j)x_j - (x_{j+1} - x_j)y_j)}{(1 + x_j^2 + y_j^2)} \right. \\ & \left. + \frac{\beta}{T} H^{cl}(x_j, y_j) \right). \end{aligned} \quad (13)$$

and  $H^{\text{cl}} : \mathbb{R}^2 \rightarrow \mathbb{R}$  is the so-called *classical Hamiltonian* whose precise form depends on the problem of interest [46]. We refer the reader to Sec. S1 in the Supplemental Material for the details of this standard calculation. We can absorb the volume element of the integral in Eq. (12) into the action by defining  $\mathcal{S}' = \mathcal{S} + 2 \sum_i \log(1 + x_i^2 + y_i^2)$ .

Note the following regarding Eq. (13): (a) The first term, a geometric phase, introduces its own sign problem into the partition function. In standard spin coherent state QMC [47], one doesn't attempt to correct this sign problem or any original sign problem contained in  $H^{\text{cl}}$ , potentially at exponential cost to the simulation algorithm; (b) Eq. (13) requires the assumption that  $y_{j+1} - y_j$  and  $x_{j+1} - x_j$  are  $\mathcal{O}(\beta/T)$ . This is not mathematically well-founded at low spins [48, 49], but can be justified at higher spins [50]; (c) Both the geometric phase, and, it will turn out, the classical Hamiltonian, have a singularity when  $x_j^2 + y_j^2 = -1$ . This causes the action to diverge in finite flow time. Such divergences are also observed when applying the Lefschetz thimble technique to fermionic models [26, 27].

*Lefschetz Thimble QMC for Spin Systems.*—When applying the Lefschetz thimble technique to spin systems using spin coherent states, the issue of divergences in the action can be resolved by noting that the holomorphic flow is gradient-dependent. Therefore, one can modify the gradient to also diverge at singularities without disturbing the thimble structure [51]; by doing so, the flow can be slowed near singularities, removing the need to tune flow times to avoid numerical blow up [52]. The new holomorphic flow then becomes:

$$\frac{dz^i}{d\tau} = e^{-2\text{Re}\mathcal{S}/\Lambda} \overline{\frac{\partial \mathcal{S}'}{\partial z^i}} \quad (14)$$

and

$$\frac{dJ_k^i}{d\tau} = e^{-2\text{Re}\mathcal{S}/\Lambda} \left[ \left\{ \overline{\frac{\partial^2 \mathcal{S}'}{\partial z^i \partial z^j}} - \frac{1}{\Lambda} \overline{\frac{\partial \mathcal{S}'}{\partial z^i}} \overline{\frac{\partial \mathcal{S}'}{\partial z^j}} \right\} \overline{J_k^j} - \frac{1}{\Lambda} \overline{\frac{\partial \mathcal{S}'}{\partial z^i}} \overline{\frac{\partial \mathcal{S}'}{\partial z^j}} J_k^j \right], \quad (15)$$

where we have assumed repeated indices are summed over and  $\Lambda$  is a parameter ideally satisfying

$$\Lambda > 2 \left| \min_{\mathbf{x}, \mathbf{y} \in \mathbb{R}^T} \text{Re}\mathcal{S}(\mathbf{x}, \mathbf{y}) \right|. \quad (16)$$

*Numerical Results.*—We test our spin coherent state Lefschetz thimble method (which we name Lefschetz Spin QMC) on two simple spin systems: a single spin-40 particle with  $\hat{H} = \hat{S}_y$ , and a frustrated spin triplet consisting of 3 spin-10 particles with  $\hat{H} = \hat{S}_{z,1}\hat{S}_{z,2} + \hat{S}_{z,2}\hat{S}_{z,3} + \hat{S}_{z,3}\hat{S}_{z,1} + \hat{S}_{x,1}\hat{S}_{x,2} + \hat{S}_{x,2}\hat{S}_{x,3} + \hat{S}_{x,3}\hat{S}_{x,1}$  [53]. The first Hamiltonian has a vanishing geometric phase, and thus has no sign problem. However, it serves as a good test

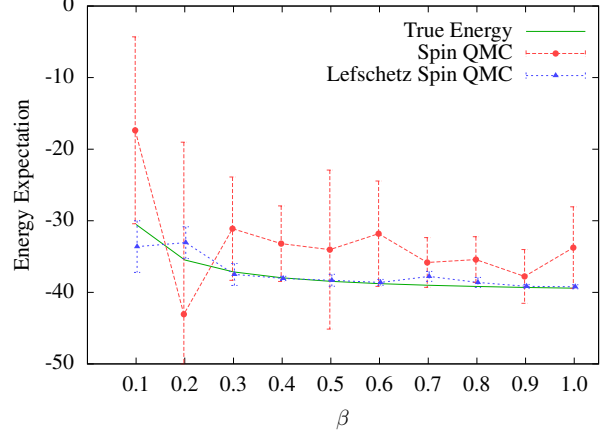


FIG. 1. We plot the performance of the Spin Quantum Monte Carlo (QMC) and Lefschetz Spin QMC in estimating the average energy of the single qubit example. The “True Energy” is the energy expectation value we would expect from the Boltzmann weights at the given inverse temperature,  $\beta$ . Note that the  $x$ -axis coordinates have been slightly shifted to make the error bars non-overlapping and more visible.

to see whether the sign problem introduced by the spin coherent state path integral can be overcome by Lefschetz Spin QMC. The second is known to have a genuine sign problem [3] and serves as a natural test case of our method's efficacy in ameliorating actual sign problems. For both examples, we compare Lefschetz Spin QMC to standard spin coherent state QMC (Spin QMC), which makes no attempt to ameliorate the sign problem; for the frustrated spin triplet we also compare to standard path integral QMC.

For each  $\beta \in \{0.1, 0.2, \dots, 1.0\}$ , we ran 5 simulations with 1000 thermalization steps and 1000 actual samples. For both examples, we let  $T = 3$ . In the single spin example, we used  $\Lambda = 80$ , a flow time of 0.01, and a mean step size of  $0.03\beta^{-1/2}$  for Lefschetz Spin QMC; for Spin QMC we used a mean step size of  $0.3\beta^{-1/2}$ . In the frustrated spin triplet example, we used  $\Lambda = 300\beta$ , a flow time of  $0.05\beta^{-3/4}$ , and a mean step size of  $0.004\beta^{-0.35}$  for Lefschetz Spin QMC; for Spin QMC we used a mean step size of  $0.08\beta^{-1/4}$ . We quantify the degree of the sign problem via the magnitude of the expected phase of the sampled quasiprobability distribution  $|\langle e^{-i\text{Im}\mathcal{S}_{\text{eff}}} \rangle|$ .

In Fig. 1, we present the main results for the single spin-40 particle case, showing the estimated energy expectation value obtained via both the Spin QMC and the Lefschetz Spin QMC. This plot also shows the energy expected for each  $\beta$  value via direct computation. In Fig. 2, we present the absolute value of the average quasiprobability phase for the same simulations. In both figures, the error bars represent the standard deviation obtained over the 5 simulation repetitions.

As stated, the sign problem in this system is not in-

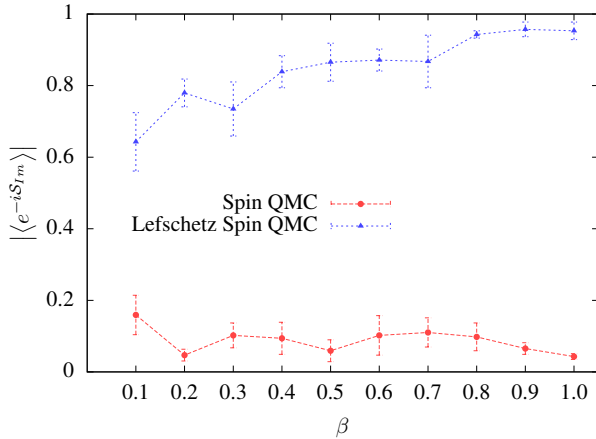


FIG. 2. We plot the performance of the Spin Quantum Monte Carlo (QMC) and Lefschetz Spin QMC by showing the expectation value of the phase of the Boltzmann weights of the corresponding classical system being sampled. A value close to zero indicates a strong sign problem with cancellation between Boltzmann weights; whereas, a value close to one indicates a weak sign problem (or no sign problem at one exactly).

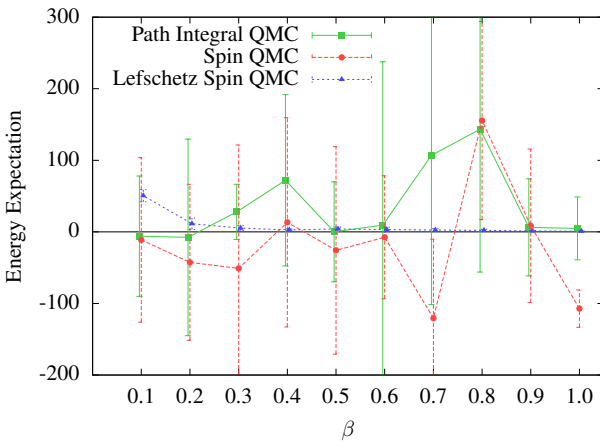


FIG. 3. We plot the performance of the Path Integral Quantum Monte Carlo (QMC), Spin QMC, and Lefschetz Spin QMC in estimating the average energy of frustrated spin triplet model. Note that the  $x$ -axis coordinates have been slightly shifted to make the error bars non-overlapping and more visible.

herent to the Hamiltonian but is introduced by the spin coherent state path integral. Our results indicate that the thimble methods are indeed capable of mitigating this sign problem.

More importantly, in Figs. 3 & 4, we present the same results for the frustrated triplet model where the sign problem is actually inherent in the model. We have included additional results from a standard path integral QMC (see Sec. S2 in the Supplemental Material for details of our implementation). For the given number of samples, both the Spin QMC and path integral QMC

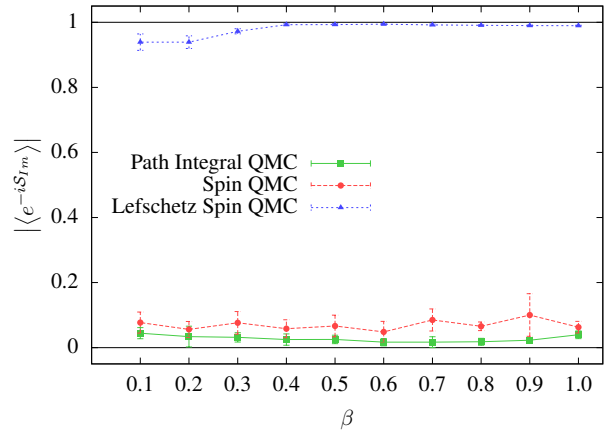


FIG. 4. We plot the performance of the Path Integral Quantum Monte Carlo (QMC), Spin QMC, and Lefschetz Spin QMC by showing the expectation value of the phase of the Boltzmann weights of the corresponding classical system being sampled. A value close to zero indicates a strong sign problem with cancellation between Boltzmann weights; whereas, a value close to one indicates a weak sign problem (or no sign problem at one exactly).

methods possess massive error bars and suffer noticeably from the sign problem; whereas, the Lefschetz Spin QMC method successfully finds the target with relatively tight error bars. As can be seen in Fig. 4, the sign problem is not being completely cured, but it is being significantly improved by these techniques.

*Conclusion and Outlook.*— These results indicate that the generalized Lefschetz thimble method is successful at mitigating the sign problem in spin systems. These numerical examples served mostly as a proof of principle of these techniques, but nothing stops them from being applicable to larger problems. The holomorphic flow does add computation time, but this time scales favorably with the size of the system and so will not introduce additional exponential factors. These methods demonstrably aid in the simulation of quantum mechanical systems, but they will not completely eliminate the sign problem in all systems, an NP-hard task. Further study is needed to find the limitations and capabilities of these techniques in larger systems and to judge the range of viability of these techniques in the low- $S$  spin limit.

*Acknowledgements.*— The research of T.C.M. was partially supported by the National Institute of Standards and Technology (NIST) Summer Undergraduate Research Fellowship (SURF) program in the Information Technology Lab (ITL). J.B. acknowledges support by the U.S. Department of Energy, Office of Science, Office of Advanced Scientific Computing Research, Department of Energy Computational Science Graduate Fellowship (award No. DE-SC0019323).

---

[1] M. Troyer and U.-J. Wiese, Computational complexity and fundamental limitations to fermionic quantum Monte Carlo simulations, *Phys. Rev. Lett.* **94**, 170201 (2005).

[2] M. Marvian, D. A. Lidar, and I. Hen, On the computational complexity of curing non-stoquastic Hamiltonians, *Nat Commun* **10**, 1571 (2019).

[3] I. Hen, Resolution of the sign problem for a frustrated triplet of spins, *Phys. Rev. E* **99**, 033306 (2019).

[4] Z.-X. Li, Y.-F. Jiang, and H. Yao, Solving the fermion sign problem in quantum Monte Carlo simulations by Majorana representation, *Phys. Rev. B* **91**, 241117 (2015).

[5] Z.-Q. Wan, S.-X. Zhang, and H. Yao, Mitigating sign problem by automatic differentiation, *arXiv: 2010.01141* (2020).

[6] D. Hangleiter, I. Roth, D. Nagaj, and J. Eisert, Easing the Monte Carlo sign problem, *Sci. Adv.* **6**, eabb8341 (2020).

[7] S. Bravyi, D. P. Divincenzo, R. I. Oliveira, and B. M. Terhal, The complexity of stoquastic local Hamiltonian problems, *arXiv:quant-ph/0606140* (2006).

[8] M. Jarret, Hamiltonian surgery: Cheeger-type gap inequalities for nonpositive (stoquastic), real, and hermitian matrices, *arXiv preprint arXiv:1804.06857* (2018).

[9] I. Hen, Determining quantum Monte Carlo simulability with geometric phases, *Phys. Rev. R.* **3**, 023080 (2021).

[10] S. Bravyi and B. Terhal, Complexity of stoquastic frustration-free hamiltonians, *Siam J. Comput.* **39**, 1462 (2010).

[11] S. Bravyi, A. J. Bessen, and B. Terhal, Merlin-arthur games and stoquastic complexity, *arXiv:quant-ph/0606140* (2006).

[12] E. Crosson and A. Harrow, Rapid mixing of path integral monte carlo for 1d stoquastic hamiltonians, *Quantum* **5**, 395 (2021).

[13] J. Bringewatt and M. Jarret, Effective gaps are not effective: Quasipolynomial classical simulation of obstructed stoquastic Hamiltonians, *Phys. Rev. Lett.* **125**, 170504 (2020).

[14] M. B. Hastings, The power of adiabatic quantum computation with no sign problem, *arXiv:2005.03791* (2020).

[15] D. Aharonov, W. Van Dam, J. Kempe, Z. Landau, S. Lloyd, and O. Regev, Adiabatic quantum computation is equivalent to standard quantum computation, *SIAM review* **50**, 755 (2008).

[16] F. Pham, Vanishing homologies and the  $n$  variable saddlepoint method, *Proc. Symp. Pure Math.* **40**, 310 (1983).

[17] E. Witten, A new look at the path integral of quantum mechanics, *Surv. Differ. Geom.* **15**, 345 (2010).

[18] E. Witten, Analytic continuation of Chern-Simons theory, *AMS/IP Stud. Adv. Math* **50**, 347 (2011).

[19] M. Cristoforetti, F. Di Renzo, and L. Scorzato, New approach to the sign problem in quantum field theories: High density QCD on a Lefschetz thimble, *Phys. Rev. D* **86**, 074506 (2012).

[20] M. Cristoforetti, F. Di Renzo, A. Mukherjee, and L. Scorzato, Monte carlo simulations on the lefschetz thimble: Taming the sign problem, *Phys. Rev. D* **88**, 051501 (2013).

[21] A. Mukherjee, M. Cristoforetti, and L. Scorzato, Metropolis Monte Carlo integration on the Lefschetz thimble: Application to a one-plaquette model, *Phys. Rev. D* **88**, 051502 (2013).

[22] H. Fujii, D. Honda, M. Kato, Y. Kikukawa, S. Komatsu, and T. Sano, Hybrid Monte Carlo on Lefschetz thimbles — a study of the residual sign problem, *J. High Energy Phys.* **2013**, 147 (2013).

[23] G. Aarts, Lefschetz thimbles and stochastic quantization: Complex actions in the complex plane, *Phys. Rev. D* **88**, 094501 (2013).

[24] M. Cristoforetti, F. Di Renzo, G. Eruzzi, A. Mukherjee, C. Schmidt, L. Scorzato, and C. Torrero, An efficient method to compute the residual phase on a Lefschetz thimble, *Phys. Rev. D* **89**, 114505 (2014).

[25] G. Aarts, L. Bongiovanni, E. Seiler, and D. Sexty, Some remarks on lefschetz thimbles and complex langevin dynamics, *J. High Energ. Phys.* **2014** (10), 1.

[26] T. Kanazawa and Y. Tanizaki, Structure of lefschetz thimbles in simple fermionic systems, *J. High Energ. Phys.* **2015** (3), 1.

[27] H. Fujii, S. Kamata, and Y. Kikukawa, Lefschetz thimble structure in one-dimensional lattice Thirring model at finite density, *J. High Energy Phys.* **2015**, 1 (2015).

[28] A. Alexandru, G. Başar, and P. Bedaque, Monte Carlo algorithm for simulating fermions on Lefschetz thimbles, *Phys. Rev. D* **93**, 014504 (2016).

[29] A. Alexandru, G. Başar, P. F. Bedaque, G. W. Ridgway, and N. C. Warrington, Monte Carlo calculations of the finite density Thirring model, *Phys. Rev. D* **95**, 014502 (2017).

[30] A. Alexandru, P. F. Bedaque, H. Lamm, S. Lawrence, and N. C. Warrington, Fermions at finite density in 2 + 1 dimensions with sign-optimized manifolds, *Phys. Rev. Lett.* **121**, 191602 (2018).

[31] F. Di Renzo and G. Eruzzi, One-dimensional qcd in thimble regularization, *Phys. Rev. D* **97**, 014503 (2018).

[32] A. Alexandru, G. Başar, P. F. Bedaque, H. Lamm, and S. Lawrence, Finite density QED<sub>1+1</sub> near Lefschetz thimbles, *Phys. Rev. D* **98**, 034506 (2018).

[33] A. Mukherjee and M. Cristoforetti, Lefschetz thimble monte carlo for many-body theories: A hubbard model study, *Phys. Rev. B* **90**, 035134 (2014).

[34] Y. Tanizaki, Y. Hidaka, and T. Hayata, Lefschetz-thimble analysis of the sign problem in one-site fermion model, *New J. Phys.* **18**, 033002 (2016).

[35] M. Ulybyshev, C. Winterowd, and S. Zafeiropoulos, Lefschetz thimbles decomposition for the hubbard model on the hexagonal lattice, *Phys. Rev. D* **101**, 014508 (2020).

[36] R. Stratovich, On a method of calculating quantum distribution functions, *Soviet Phys. Doklady* **2**, 416 (1958).

[37] J. Hubbard, Calculation of partition functions, *Phys. Rev. Lett.* **3**, 77 (1959).

[38] P. A. Mishchenko, Y. Kato, and Y. Motome, A quantum Monte Carlo method on asymptotic Lefschetz thimbles for quantum spin systems: An application to the Kitaev model in a magnetic field, *arXiv:2106.07937* (2021).

[39] F. Di Renzo and G. Eruzzi, Thimble regularization at work: From toy models to chiral random matrix theories, *Phys. Rev. D* **92**, 085030 (2015).

[40] A. Alexandru, G. Başar, P. F. Bedaque, G. W. Ridgway, and N. C. Warrington, Sign problem and monte carlo calculations beyond lefschetz thimbles,

*J. High Energ. Phys.* **2016** (5), 1.

[41] M. Fukuma and N. Umeda, Parallel tempering algorithm for integration over Lefschetz thimbles, *Prog. Theor. Exp. Phys.* **2017**, 073B01 (2017).

[42] A. Alexandru, G. Başar, P. F. Bedaque, and G. Ridgway, Schwinger-Keldysh formalism on the lattice: A faster algorithm and its application to field theory, *Phys. Rev. D* **95**, 114501 (2017).

[43] A. Alexandru, G. Başar, P. F. Bedaque, and N. C. Warrington, Complex Paths Around The Sign Problem, *arXiv:2007.05436* (2020).

[44] A. Alexandru, G. Başar, P. F. Bedaque, G. W. Ridgway, and N. C. Warrington, Fast estimator of Jacobians in the Monte Carlo integration on Lefschetz thimbles, *Phys. Rev. D* **93**, 094514 (2016).

[45] J. M. Radcliffe, Some properties of coherent spin states, *J. Phys. A: Gen. Phys.* **4**, 313 (1971).

[46] E. Kochetov, SU(2) coherent-state path integral, *J. Math. Phys.* **36**, 4667 (1995).

[47] H. Takano, Monte Carlo method for quantum spin systems based on the Bloch coherent state representation, *Prog. Theor. Phys.* **73**, 332 (1985).

[48] J. Shibata and S. Takagi, A note on (spin-) coherent-state path integral, *Int. J. Mod. Phys. B* **13**, 107 (1999).

[49] A. Auerbach, *Interacting Electrons and Quantum Magnetism* (Springer-Verlag, 1994).

[50] A. Garg, E. Kochetov, K.-S. Park, and M. Stone, Spin coherent-state path integrals and the instanton calculus, *arXiv:cond-mat/0111139* (2001).

[51] Y. Tanizaki, H. Nishimura, and J. J. M. Verbaarschot, Gradient flows without blow-up for Lefschetz thimbles, *J. High Energy Phys.* **2017**, 100 (2017).

[52] Note that Eq. (14) and Eq. (15) correspond to taking  $\Lambda_F \rightarrow \infty$  in equations 3.1 and B.7 of [51] respectively. Furthermore, we are letting  $\mathcal{S}_B = \mathcal{S}$  and the  $\mathcal{S}$  of [51] be our  $\mathcal{S}'$ . Hence, in our code, we call  $\mathcal{S}$  the bosonic action (where the  $B$  comes from in [51]), and  $\mathcal{S}'$  just the action.

[53] The code used for implementing this is at: <https://github.com/Connor-Mooney/LTMC-Spin-Systems>. Note that the triplet is implemented in `Spin_System.py`, the single spin in `Single_Spin_System.py`, and the triplet with standard Path integral QMC in `Triplet_Naive_PIMC.py`. However, `Spin_System.py` should be able to implement arbitrary spin systems if the appropriate hamiltonian class is created for the system.

## SUPPLEMENTAL MATERIAL FOR: LEFSCHETZ THIMBLE QUANTUM MONTE CARLO FOR SPIN SYSTEMS

In this Supplemental Material, we derive the spin coherent state path integral (Sec. S1) and specify the details of our numerical implementation of standard path integral quantum Monte Carlo for the example of the frustrated spin triplet (Sec. S2)

## CONTENTS

|  |    |
|--|----|
| S1. Derivation of Spin Coherent State Path Integral  | 7  |
| The Partition Function                               | 7  |
| Classical Hamiltonian Elements                       | 9  |
| Multi-particle Systems                               | 10 |
| S2. Path Integral Quantum Monte Carlo Implementation | 10 |

### S1. DERIVATION OF SPIN COHERENT STATE PATH INTEGRAL

#### The Partition Function

To derive the spin coherent state path integral, we begin with the definition of the partition function:

$$\mathcal{Z} = \text{Tr}\{e^{-\beta \hat{H}}\}.$$

We restate the spin coherent state resolution of the identity here for convenience

$$I = \frac{2S+1}{\pi} \int_{\mathbb{R}^2} \frac{d^2\mu}{(1+|\mu|^2)^2} |\mu\rangle \langle \mu|. \quad (\text{S.1})$$

Now, as  $\hat{H}$  commutes with itself, we can insert the spin coherent state resolution of the identity from Eq. (S.1) between each imaginary-time step and rewrite this expression as

$$\begin{aligned} \mathcal{Z} &= \text{Tr} \left\{ \left( e^{-(\beta/T)\hat{H}} \right)^T \right\} \\ &= \text{Tr} \left\{ \left( e^{-(\beta/T)\hat{H}} \left( \frac{2S+1}{\pi} \int_{\mathbb{R}^2} \frac{d^2\mu}{(1+|\mu|^2)^2} |\mu\rangle \langle \mu| \right) \right)^T \right\} \\ &= \left( \prod_{j=0}^{T-1} \frac{2S+1}{\pi} \int_{\mathbb{R}^2} \frac{d^2\mu_j}{(1+|\mu_j|^2)^2} \right) \left( \prod_{j=0}^{T-1} \langle \mu_{j+1} | e^{-\frac{\beta}{T}\hat{H}} | \mu_j \rangle \right) \end{aligned} \quad (\text{S.2})$$

where, enforcing the periodicity imposed by the trace, we have  $\mu_T = \mu_0$ . Next we expand the exponential out to first order in  $\beta/T$  and get that

$$\begin{aligned} \langle \mu_{j+1} | e^{-\frac{\beta}{T}\hat{H}} | \mu_j \rangle &= \langle \mu_{j+1} | \left( I - \frac{\beta}{T}\hat{H} + \mathcal{O} \left( \left( \frac{\beta}{T} \right)^2 \right) \right) | \mu_j \rangle \\ &= \langle \mu_{j+1} | \mu_j \rangle \left( 1 - \frac{\beta}{T} H^{cl}(\bar{\mu}_{j+1}, \mu_j) + \mathcal{O} \left( (\beta/T)^2 \right) \right), \end{aligned}$$

where  $H^{cl}(\bar{\mu}_{j+1}, \mu_j) \equiv \langle \mu_{j+1} | H | \mu_j \rangle / \langle \mu_{j+1} | \mu_j \rangle$  will be examined in detail in the next section. Now, using that the overlap of two spin coherent states  $|\mu\rangle$  and  $|\mu'\rangle$  is  $\langle \mu' | \mu \rangle = (1 + \bar{\mu}'\mu)^{2S} / ((1 + |\mu|^2)(1 + |\mu'|^2))^S$  [45], we can rewrite this expression as

$$\frac{(1 + \bar{\mu}_{j+1}\mu_j)^{2S}}{((1 + |\mu_{j+1}|^2)(1 + |\mu_j|^2))^S} \left( 1 - (\beta/T) H^{cl}(\bar{\mu}_{j+1}, \mu_j) + \mathcal{O} \left( (\beta/T)^2 \right) \right)$$

The next task is to simplify the inner product in front. To make this possible, we make the standard assumption in deriving path integral expansions that  $|\mu_{j+1} - \mu_j| \equiv |\delta_{j+1}| = \mathcal{O}(\beta/T)$ . There is analytical evidence that this assumption is not mathematically well-founded for spin-coherent state path integrals [48–50], but we, like much of the literature making use of this technique, shall proceed despite that. Thus, making that assumption, we can write that

$$\frac{(1 + \bar{\mu}_{j+1}\mu_j)^{2S}}{((1 + |\mu_{j+1}|^2)(1 + |\mu_j|^2))^S} = 1 - \frac{((1 + |\mu_{j+1}|^2)(1 + |\mu_j|^2))^S - (1 + \bar{\mu}_{j+1}\mu_j)^{2S}}{((1 + |\mu_{j+1}|^2)(1 + |\mu_j|^2))^S} \quad (\text{S.3})$$

$$= 1 + S \frac{(\bar{\delta}_{j+1}\mu_j - \delta_{j+1}\bar{\mu}_j)(1 + |\mu_j|^2)^{2S-1}}{((1 + |\mu_{j+1}|^2)(1 + |\mu_j|^2))^S} + \mathcal{O}((\beta/T)^2) \quad (\text{S.4})$$

$$= 1 + S \frac{(\bar{\delta}_{j+1}\mu_j - \delta_{j+1}\bar{\mu}_j)}{(1 + |\mu_j|^2)} + \mathcal{O}((\beta/T)^2), \quad (\text{S.5})$$

where to get between the first and second, as well as second and third lines we use the binomial expansion.

Multiplying these two together, we finally get that

$$\begin{aligned} \langle \mu_{j+1} | e^{-\beta H/T} | \mu_j \rangle &= 1 + S \frac{(\bar{\delta}_{j+1}\mu_j - \delta_{j+1}\bar{\mu}_j)}{(1 + |\mu_j|^2)} - \frac{\beta}{T} H^{cl}(\bar{\mu}_{j+1}, \mu_j) + \mathcal{O} \left( \left( \frac{\beta}{T} \right)^2 \right) \\ &= \exp \left\{ S \frac{(\bar{\delta}_{j+1}\mu_j - \delta_{j+1}\bar{\mu}_j)}{(1 + |\mu_j|^2)} - \frac{\beta}{T} H^{cl}(\bar{\mu}_j, \mu_j) \right\} + \mathcal{O} \left( \left( \frac{\beta}{T} \right)^2 \right). \end{aligned} \quad (\text{S.6})$$

Plugging this back into Eq. (S.2), we get that

$$\mathcal{Z} = \left( \prod_{j=0}^{T-1} \frac{2S+1}{\pi} \int_{\mathbb{R}^2} \frac{d^2\mu_j}{(1+|\mu_j|^2)^2} \right) e^{-\mathcal{S}[\{\mu_j\}]} + \mathcal{O}(\beta/T), \quad (\text{S.7})$$

where

$$\mathcal{S}[\{\mu_j\}] \equiv \sum_{j=0}^{T-1} \left( -S \frac{(\bar{\delta}_{j+1}\mu_j - \delta_{j+1}\bar{\mu}_j)}{(1+|\mu_j|^2)} + \frac{\beta}{T} H^{cl}(\bar{\mu}_j, \mu_j) \right). \quad (\text{S.8})$$

Letting  $x \equiv \text{Re}\mu$  and  $y \equiv \text{Im}\mu$ , we arrive at

$$\mathcal{Z} = \left( \prod_{j=0}^{T-1} \frac{2S+1}{\pi} \int_{\mathbb{R}^2} \frac{dx_j dy_j}{(1+x_j^2+y_j^2)^2} \right) e^{-\mathcal{S}[\{x_j\}, \{y_j\}]} + \mathcal{O}(\beta/T), \quad (\text{S.9})$$

$$\mathcal{S}[\{x_j\}, \{y_j\}] \equiv \sum_{j=0}^{T-1} \left( 2iS \frac{((y_{j+1}-y_j)x_j - (x_{j+1}-x_j)y_j)}{(1+x_j^2+y_j^2)} + \frac{\beta}{T} H^{cl}(\bar{\mu}_j, \mu_j) \right). \quad (\text{S.10})$$

This action is similar to that of [46], but, importantly for our purposes, has no singularities over  $\mathbb{R}^{2T}$ . Only when this action is continued to  $\mathbb{C}^{2T}$  will singularities emerge.

To get the continuum limit, which we do not actually use in our analysis, but is nevertheless the most compact and aesthetically pleasing way of presenting the path integral, we then take  $T \rightarrow \infty$  and notice that as  $\delta_j = \mathcal{O}(\beta/T)$  by assumption, we can define derivatives with respect to that parameter. Thus, we get that

$$\mathcal{Z} = \int \mathcal{D}x \mathcal{D}y e^{-\mathcal{S}[x, y]}, \quad (\text{S.11})$$

where

$$\mathcal{S}[x, y] = \int_0^\tau d\tau \left( 2iS \frac{\dot{y}x - \dot{x}y}{1+x^2+y^2} + H^{cl}(x, y) \right), \quad (\text{S.12})$$

and  $H^{cl}(x, y) \equiv H^{cl}(x - iy, x + iy)$ .

### Classical Hamiltonian Elements

One thing that we have not done yet is calculate  $H^{cl}(x, y)$  explicitly. To do this, notice that  $|\uparrow\rangle = (|+1/2\rangle)^{\otimes 2S}$  and that

$$\begin{aligned} \hat{S}_- = & (\hat{\sigma}_x - i\hat{\sigma}_y) \otimes I^{\otimes(2S-1)} + I \otimes (\hat{\sigma}_x - i\hat{\sigma}_y) \otimes I^{\otimes(2S-2)} \\ & + \cdots + I^{\otimes 2S-1} \otimes (\hat{\sigma}_x - i\hat{\sigma}_y). \end{aligned} \quad (\text{S.13})$$

The definition of a spin coherent state is

$$|\mu\rangle = \frac{1}{(1+|\mu|^2)^S} \exp\{\mu\hat{S}_-\} |\uparrow\rangle. \quad (\text{S.14})$$

Plugging Eq. (S.13) and the definition of  $|\uparrow\rangle$  into Eq. (S.14), we can utilize the commutivity of the terms in Eq. (S.13) to get that

$$|\mu\rangle = \frac{1}{(1+|\mu|^2)^S} \bigotimes_1^{2S} (\exp\{\mu(\hat{\sigma}_x - i\hat{\sigma}_y)\} |+1/2\rangle).$$

We can write out the state in the spin-1/2 space explicitly, using that  $(\hat{\sigma}_x - i\hat{\sigma}_y)^2 = 0$ , to obtain that

$$(\exp\{\mu(\hat{\sigma}_x - i\hat{\sigma}_y)\} |+1/2\rangle) = |+1/2\rangle + \mu | -1/2\rangle.$$

Now, let  $\mu \equiv x + iy$ , and notice that we can write  $\hat{S}_x$ ,  $\hat{S}_y$ , and  $\hat{S}_\mu$  in the same way as  $\hat{S}_-$ . Thus, We can use this expression to finally get the classical Hamiltonians corresponding to the spin operators:

$$\hat{S}_x : H^{cl}(x, y) = 2S \frac{x}{1+x^2+y^2} \quad (\text{S.15})$$

$$\hat{S}_y : H^{cl}(x, y) = 2S \frac{y}{1+x^2+y^2} \quad (\text{S.16})$$

$$\hat{S}_z : H^{cl}(x, y) = S \frac{1-x^2-y^2}{1+x^2+y^2}. \quad (\text{S.17})$$

### Multi-particle Systems

Adapting the above derivations to systems with multiple particles is straightforward. Doing so, we get that for an  $n$ -particle system the path integral is:

$$\mathcal{Z} = \int \left( \prod_{j=1}^n \mathcal{D}x^{(j)} \mathcal{D}y^{(j)} \right) e^{-\mathcal{S}[\{x^{(j)}\}, \{y^{(j)}\}]} \quad (\text{S.18})$$

where

$$\mathcal{S}[\{x^{(j)}\}, \{y^{(j)}\}] = \int_0^\tau d\tau \left( 2iS \sum_{j=1}^n \frac{\dot{y}^{(j)}x^{(j)} - \dot{x}^{(j)}y^{(j)}}{1 + (x^{(j)})^2 + (y^{(j)})^2} + H^{\text{cl}}(\{x^{(j)}\}, \{y^{(j)}\}) \right)$$

and  $H^{\text{cl}}(\{x^{(j)}\}, \{y^{(j)}\})$  is obtained by replacing  $\hat{S}_a$  acting on the  $j^{\text{th}}$  particle by its corresponding single-particle classical Hamiltonian  $H^{\text{cl}}(x^{(j)}, y^{(j)})$ , i.e.

$$\hat{S}_z \otimes \hat{S}_x \rightarrow \left( S \frac{1 - (x^{(1)})^2 - (y^{(1)})^2}{1 + (x^{(1)})^2 + (y^{(1)})^2} \right) \left( \frac{2Sx^{(2)}}{1 + (x^{(2)})^2 + (y^{(2)})^2} \right).$$

## S2. PATH INTEGRAL QUANTUM MONTE CARLO IMPLEMENTATION

To do path integral Quantum Monte Carlo on a frustrated triplet with Hamiltonian

$$\hat{H} = \hat{S}_{1,z}\hat{S}_{2,z} + \hat{S}_{2,z}\hat{S}_{3,z} + \hat{S}_{1,z}\hat{S}_{3,z} + \hat{S}_{1,x}\hat{S}_{2,x} + \hat{S}_{2,x}\hat{S}_{3,x} + \hat{S}_{1,x}\hat{S}_{3,x}, \quad (\text{S.19})$$

we decompose  $\hat{H}$  into a diagonal and off-diagonal part with  $\hat{H}_d \equiv \hat{S}_{1,z}\hat{S}_{2,z} + \hat{S}_{2,z}\hat{S}_{3,z} + \hat{S}_{1,z}\hat{S}_{3,z}$  and  $\hat{H}_o \equiv \hat{S}_{1,x}\hat{S}_{2,x} + \hat{S}_{2,x}\hat{S}_{3,x} + \hat{S}_{1,x}\hat{S}_{3,x}$  respectively. We then use the approximation

$$\begin{aligned} e^{-\beta(\hat{H}_d + \hat{H}_o)} &= \left( e^{-\beta(\hat{H}_d + \hat{H}_o)/T} \right)^T \\ &\approx \left( e^{-\beta\hat{H}_d/T} e^{-\beta\hat{H}_o/T} \right)^T, \end{aligned} \quad (\text{S.20})$$

for large  $T$ .

Now, we insert resolutions of the identity in the  $z$ -basis around each exponential of the diagonal Hamiltonian, and resolutions of the identity in the  $x$ -basis around each off-diagonal to get

$$\begin{aligned} e^{-\beta(\hat{H}_d + \hat{H}_o)} &\approx \sum_{z_0, \dots, z_{T-1}, x_0, \dots, x_{T-1}} |z_0\rangle \langle z_0| e^{-\beta\hat{H}_d/T} |z_0\rangle \langle z_0| x_0 \rangle \langle x_0| e^{-\beta\hat{H}_o/T} |x_0\rangle \langle x_0| z_1 \rangle \dots \\ &\quad \times \langle z_{T-1}| x_{T-1} \rangle \langle x_{T-1}| e^{-\beta\hat{H}_o/T} |x_{T-1}\rangle \langle x_{T-1}|. \end{aligned} \quad (\text{S.21})$$

Taking the trace, we get that

$$\begin{aligned} \mathcal{Z} &= \text{Tr}\{e^{-\beta\hat{H}}\} \\ &\approx \sum_{z_0, \dots, z_{T-1}, x_0, \dots, x_{T-1}} \langle z_0| e^{-\beta\hat{H}_d/T} |z_0\rangle \langle z_0| x_0 \rangle \langle x_0| e^{-\beta\hat{H}_o/T} |x_0\rangle \langle x_0| z_1 \rangle \dots \langle z_{T-1}| x_{T-1} \rangle \langle x_{T-1}| e^{-\beta\hat{H}_o/T} |x_{T-1}\rangle \langle x_{T-1}| z_0 \rangle \\ &= \sum_{z_0, \dots, z_{T-1}, x_0, \dots, x_{T-1}} \prod_{j=0}^{T-1} \langle z_j| e^{-\beta\hat{H}_d/T} |z_j\rangle \langle z_j| x_j \rangle \langle x_j| e^{-\beta\hat{H}_o/T} |x_j\rangle \langle x_j| z_{j+1} \rangle, \end{aligned}$$

where  $z_T \equiv z_0$  and  $x_0 \equiv x_T$ . At low spins, it is often not too difficult to explicitly calculate the sum over the  $x_j$  variables. However, this quickly becomes unfeasible. As such, we sampled over values of both  $x_j$  and  $z_j$ .

To carry out the Metropolis algorithm, we sweep through the  $x_j$  and  $z_j$  variables in order, proposing and testing a randomly chosen new value for each dit before moving on to the next. Each proposal involves a simultaneous proposed change for  $z_j$  and the corresponding  $x_j$ . In the main text when we report the number of thermalization steps and samples for the Monte Carlo algorithm, each “step” of the path integral QMC is a full sweep of proposed changes to every  $x_j$  and  $z_j$  variable.